Seasonal Clear-sky Flux and Cloud Radiative Effect Anomalies in the Arctic Atmospheric Column Associated with the Arctic Oscillation and Arctic Dipole

Bradley M. Hegyi[1, a)] and Patrick C. Taylor[1, b)]

[1]NASA Langley Research Center, Hampton, VA

[a)]*Corresponding author: bradley.m.hegyi@nasa.gov*
[b)]*patrick.c.taylor@nasa.gov*

Abstract. The impact of the Arctic Oscillation (AO) and Arctic Dipole (AD) on the radiative flux into the Arctic mean atmospheric column is quantified. 3-month-averaged AO and AD indices are regressed with corresponding surface and top-of-atmosphere (TOA) fluxes from the CERES-SFC and CERES-TOA EBAF datasets over the period 2000-2014. An increase in clear-sky fluxes into the Arctic mean atmospheric column during fall is the largest net flux anomaly associated with AO, primarily driven by a positive net longwave flux anomaly (i.e. increase of net flux into the atmospheric column) at the surface. A decrease in the Arctic mean atmospheric column cloud radiative effect during winter and spring is the largest flux anomaly associated with AD, primarily driven by a change in the longwave cloud radiative effect at the surface. These prominent responses to AO and AD are widely distributed across the ice-covered Arctic, suggesting that the physical process or processes that bring about the flux change associated with AO and AD are distributed throughout the Arctic.

INTRODUCTION

The net radiative flux into the atmospheric column at the top and bottom of the atmosphere is a crucial component of the energy budget of the Arctic atmosphere, as part of the overall Arctic energy balance.[1] The magnitude of the radiative flux at the top and bottom of the Arctic atmospheric column is affected by changes in cloud properties (i.e. cloud radiative effects), as well as changes within the atmospheric column independent of clouds (i.e. clear-sky effects). At the surface, longwave and shortwave flux anomalies are a primary mechanism by which atmospheric variability interacts with the surface energy budget, and subsequently sea ice variability during both the melt and freeze-up of sea ice.[2,3] Changes in the characteristics of clouds and the atmospheric column have been linked to large-scale atmospheric variability in the Arctic. Arctic large-scale atmospheric variability is characterized by preferred modes, or patterns, of variability. Two such patterns are the Arctic Oscillation (AO) and Arctic Dipole (AD).[4,5] Both the AO and AD have been linked to atmospheric temperature and water vapor content anomalies and cloud vertical and horizontal distribution and thus have the potential to affect surface and top-of-atmosphere (TOA) radiative fluxes.[6]

Given the potential and established links between atmospheric variability and radiative fluxes in Arctic atmospheric column, the purpose of this paper is to quantify the impacts of AO and AD on longwave and shortwave radiative fluxes at the top and bottom of the Arctic atmospheric column in all seasons. The results presented are a first step toward better understanding the physical mechanism that links large-scale atmospheric variability to changes in the Arctic energy budget.

DATA AND METHODS

For all surface and TOA radiative flux quantities, we use NASA Clouds and the Earth's Radiant Energy System Energy Balanced and Filled monthly data (CERES EBAF-Surface[TOA]_Ed2.8), on a 1-degree latitude by 1-degree longitude grid.[7] Both the AO and AD are circulation patterns defined as the result of the application of principal

component analysis on Northern Hemisphere sea level pressure and near-surface geopotential height. The AO is defined as the leading empirical function (EOF) of 1000 mb geopotential height north of 20°N latitude.[8] We use the monthly AO index from the Climate Prediction Center (CPC). The AD is defined as the second EOF of 1000mb geopotential height north of 70°N latitude.[9] We calculate the AD index using this definition and NCEP-NCAR reanalysis data.[10]

To capture the seasonal response of the surface and TOA fluxes, we regress the 3-month average atmospheric column fluxes with corresponding 3-month-average AO and AD indices at each grid point in the CERES-EBAF data over the 2000-2014 period. The atmospheric column flux is the sum of the net incoming flux at TOA and net upward flux at the surface, and is directly related to the heating or cooling of the atmospheric column.[1] To account for the inherent trend in some of the flux quantities over this period (e.g. upwelling shortwave flux) and focus on the interannual variability, we detrend the CERES-EBAF data before regressing with the AO and AD indices.

RESULTS

We present the Arctic mean net clear-sky flux and cloud radiative effect anomalies associated with the Arctic Oscillation (AO) and Arctic Dipole (AD) for each 3-month averaging period (DJF: winter, December-February, MAM: spring, March-May, JJA: summer, June-August, SON: fall, September-November) in Table 1. Positive (negative) values indicate a net flux into (out of) the atmospheric column that warms (cools) the column. The largest magnitude net radiative flux anomaly associated with the AO is found in the fall (SON), with a clear-sky net flux increase of 2.5 W m^{-2}. An associated positive clear-sky flux anomaly also exists in winter, and an associated negative clear-sky flux anomaly exists in summer. The cloud radiative effect associated with AO is near zero or positive in all seasons, with the largest associated cloud effect in spring. Overall, the all-sky mean response to AO, which is the sum of the associated clear-sky flux and cloud radiative effect anomalies, is positive in all seasons except for summer, meaning that the total radiative flux anomalies associated with a positive AO index tend to warm the Arctic mean atmospheric column.

TABLE 1. Arctic-average net clear-sky flux anomalies and net cloud radiative effect (CRE) anomalies for the atmospheric column, associated with 3-month averaged AO and AD indices from 2000-2014 (units: W m-2). Arctic average is defined as all areas north of 65 degrees North latitude. Associated anomalies are determined by linear regression between time series of 3-month-averaged CERES-EBAF fluxes and 3-month-averaged AO/AD indices. Positive (negative) numbers refer to net warming (cooling) of the atmospheric column by corresponding net radiative flux anomalies.

	DJF	**DJF**	**MAM**	**MAM**	**JJA**	**JJA**	**SON**	**SON**
Flux Type	***Clear-Sky***	***CRE***	***Clear-Sky***	***CRE***	***Clear-Sky***	***CRE***	***Clear-Sky***	***CRE***
AO	1.17	-0.05	0.06	0.73	-1.78	0.07	2.46	0.54
AD	-0.54	-1.62	1.33	-2.52	-0.30	0.57	0.62	-0.76

Compared to the AO, the cloud radiative effect anomalies associated with AD are much more dominant than the associated clear-sky anomalies in the Arctic average. A positive AD index is associated with a negative net column cloud radiative effect anomaly in all seasons outside of summer. The magnitude of the AO-associated spring cloud radiative effect anomaly is of similar magnitude as the AO-associated clear-sky flux anomaly in fall. The large negative cloud effect anomaly in spring is counteracted partially by the clear-sky flux response, thus the largest all-sky atmospheric column response to AD is in winter (-2.2 W m^{-2}). Opposite to the AO, a positive AD in all seasons but summer results in a net all-sky flux out of the atmospheric column and a cooling of the Arctic mean atmospheric column.

We now breakdown the total net clear-sky and cloud radiative effect anomalies into longwave (LW) and shortwave (SW) components, and further separate by surface and TOA in Fig. 1, to find the component that most contributes the largest clear-sky flux and cloud radiative effect anomalies shown in Table 1. The large AO-associated clear-sky flux anomaly is primarily due to a positive net LW flux at the surface (i.e. an increased net LW flux into the column at the surface), with minor contributions from net LW flux at TOA and net SW flux at the surface (Fig. 1a). Net LW flux anomalies at the surface also primarily contribute to the total positive net clear-sky flux in winter and to the total negative net clear-sky flux in summer. There is much cancellation between components in the AO-associated cloud radiative effect anomalies (Fig. 1b), explaining the small Arctic mean cloud effect values.

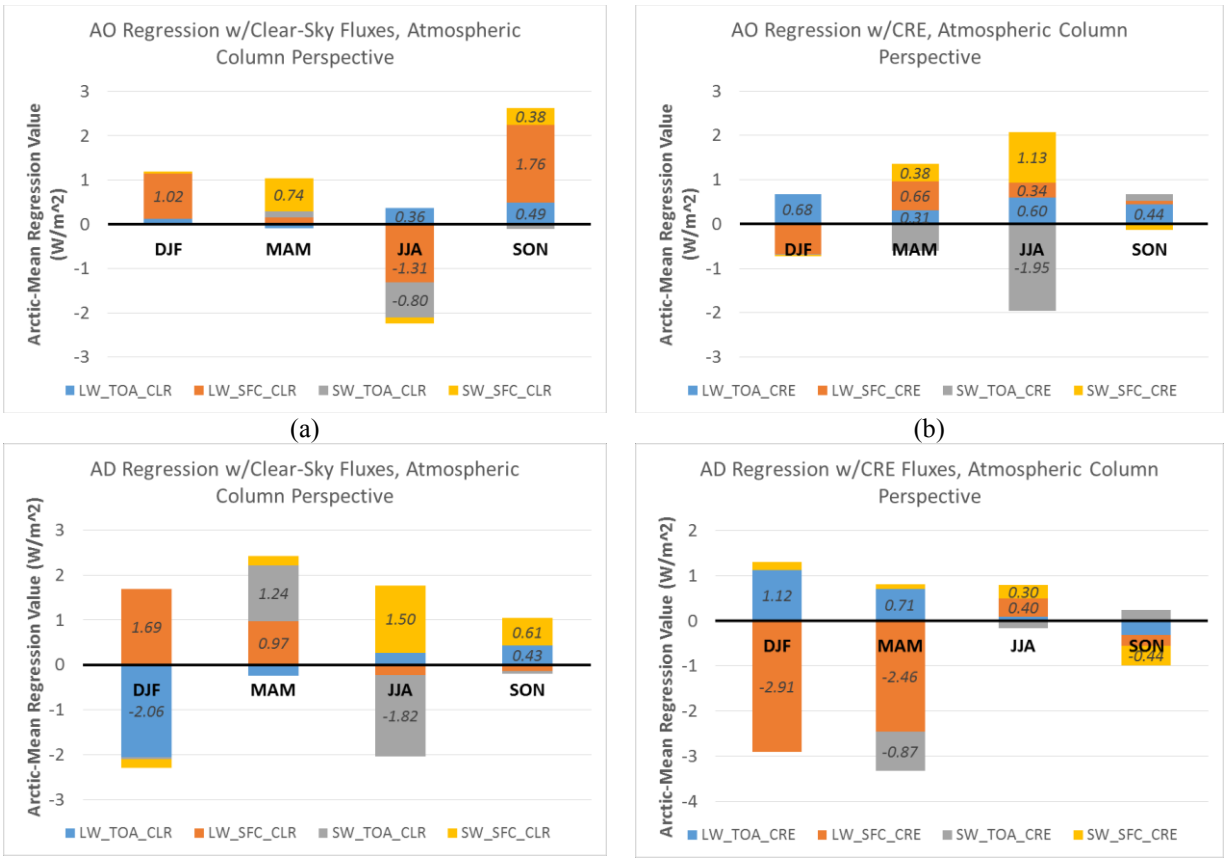

FIGURE 1. Net shortwave and longwave flux components of the Arctic-average (north of 65°N) net column radiative flux associated with AO and AD (units: W m-2). Clear-sky components are shown in panels a) and c) and cloud radiative flux components are shown in panels b) and d).

Like the AO-associated Arctic mean cloud radiative effect anomalies, there is much cancellation between components in the AD-associated clear-sky flux anomalies (Fig. 1c). The largest clear-sky response to AD in spring is primarily driven by anomalous clear sky net LW fluxes at the surface and anomalous net TOA SW fluxes. The large AD-associated cloud radiative effect anomalies in winter and spring are primarily driven by large negative net surface LW fluxes, partially counteracted by smaller positive net LW TOA flux anomalies (Fig. 1d). In the summer and fall, the cloud radiative effect response is of much smaller magnitude.

The greatest difference between the largest AO- and AD-associated anomalies are that the largest AO-associated anomalies are clear-sky flux anomalies, while the largest AD-associated anomalies are cloud radiative effect anomalies. In both cases, the largest seasonal responses to AO and AD involve LW fluxes.

The AO-associated column net positive clear-sky LW anomalies are distributed across most of the Arctic (Fig. 2a). Exceptions include the ice-free parts of the Arctic east of Greenland and north of Scandinavia. For the AD-associated longwave cloud radiative effect response in spring, the negative response is similarly distributed across most of the ice-covered portions of the Arctic (Fig. 2b). The widespread coverage of regression values that match the sign of the mean Arctic response in both cases hint that the physical process or processes that bring about the flux change are distributed throughout the Arctic. Additionally, Fig. 2 shows that the Arctic mean is not dominated by very large flux responses in a limited region of the Arctic.

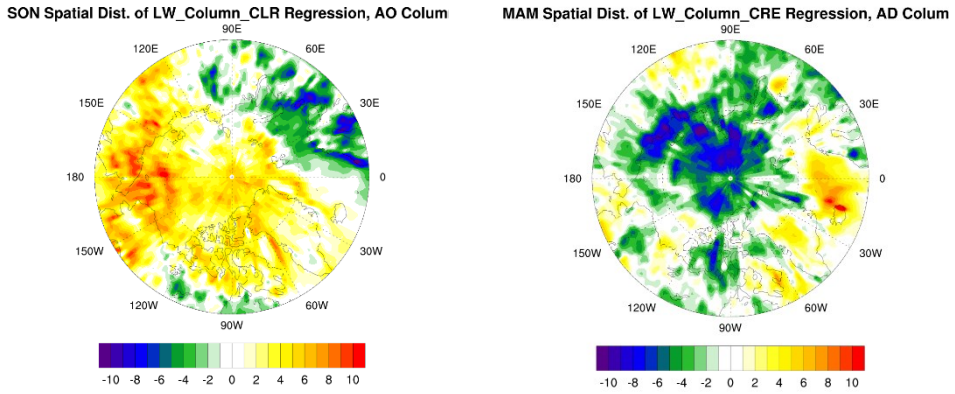

(a) (b)

FIGURE 2. a) Atmospheric column clear sky net LW flux anomaly associated with SON AO index over 2000-2014 (units: W m-2). b) Same as panel a), but longwave cloud radiative effect anomaly associated with the MAM AD index is shown.

SUMMARY AND CONCLUSIONS

By regressing CERES-EBAF seasonal-mean (i.e. DJF, MAM, JJA, and SON) flux data at the surface and the top of atmosphere with the corresponding mean Arctic Oscillation (AO) and Arctic Dipole (AD) indices, we determined the flux anomalies linearly associated with AO and AD in each season. We presented the results as the change in flux into the atmospheric column, directly related to the heating and cooling of the atmospheric column.

The largest magnitude atmospheric column clear-sky flux or cloud radiative effect anomaly associated with AO is found in fall (2.5 W m^{-2}, Table 1). The primary contributor to this positive flux anomaly is the net surface LW flux, with minor contributions from the net TOA LW flux and net surface SW flux (Figs. 1a and 1b). The largest associated clear-sky or cloud radiative effect anomaly associated with AD is in spring (-2.5 W m^{-2}, Table 1), primarily driven by the surface LW cloud radiative effect anomaly (Fig. 1d). The spatial distribution of these largest associated anomalies (Fig. 2) reveal that same-signed anomalies are found throughout the ice-covered part of the Arctic region. These results show the dominance of LW flux anomalies associated with AO and AD. A question for future work and a topic of a forthcoming paper is what physical processes lead to these LW flux anomalies.

ACKNOWLEDGMENTS

Funding for B.M. Hegyi was provided through the NASA Postdoctoral Program. CERES data were obtained from the NASA Langley Research Center CERES ordering tool at (http://ceres.larc.nasa.gov/). Funding for P. C. Taylor was provided by the NASA Interdisciplinary Studies Program grant NNH12ZDA001N-IDS.

REFERENCES

1. N. Nakamura and A.H. Oort, J. Geophys. Res. **93**, 9510-9524 (1988).
2. J.E. Kay and T.L. L'Ecuyer, J. Geophys. Res. **118**, 7219-7236 (2013).
3. Y. Liu and J.R. Key, Environ. Res. Letters **9**, 044022 (2014).
4. D.W.J. Thompson and J.M. Wallace, J. Climate **13**, 1000-1016 (2000).
5. B. Wu, J. Wang, and J.E. Walsh, J. Climate **19**, 210-225 (2006).
6. Y. Li, D.W.J. Thompson, Y. Huang, and M. Zhang, Geo. Res. Letters **41**, 1681-1688 (2014).
7. S. Kato, N. G. Loeb, F. G. Rose, D. R. Doelling, D. A. Rutan, T. E. Caldwell, L. Yu, and R. A. Weller, J. Climate **26**, 2719-2740 (2013).
8. D.W.J. Thompson and J.M. Wallace, Geo. Res. Letters **25**, 1297-1300 (1998).
9. E. Kalnay et al., BAMS **77**, 437-471 (1996).